

Thermodynamic and Structural Investigations of Ammonium Borohydride, a Solid with a Highest Content of Thermodynamically and Kinetically Accessible Hydrogen

Abhijeet Karkamkar,[†] Shawn M. Kathmann,[†]
Gregory K. Schenter,[†] David J. Heldebrant,[‡]
Nancy Hess,[†] Maciej Gutowski,[‡] and Tom Autrey^{*,†}

[†]Pacific Northwest National Laboratory, Richland, Washington 99354, and [‡]Chemistry, School of Engineering and Physical Sciences, Herriot Watt University, Edinburgh EH14 4AS, United Kingdom

Received August 3, 2009

Revised Manuscript Received August 31, 2009

Hydrogen storage is one of the most challenging technical barriers in the implementation of a hydrogen-based energy economy.^{1–3} In the pursuit of practical hydrogen storage systems, the chemical and physical properties of many complex hydrides, e.g., metal-amides, alanates, and boronates, with high hydrogen content, have been re-examined during the past decade.^{4–11} It is believed that new breakthroughs in the development of complex hydrides as practical hydrogen storage materials will benefit from knowledge of the thermodynamic properties of the reactants, products and key intermediates formed in the dehydrogenation reaction pathways.^{12–14} As such, it is notable that there has been little reported insight on the chemical and physical properties describing the solid compound with a highest gravimetric hydrogen density, ammonium borohydride $[\text{NH}_4]^+[\text{BH}_4]^-$, ca. 24 wt % hydrogen, first prepared more than 50 years ago.¹⁵ Parry et al. reported that the compound decomposed at room

temperature and that NH_4^+ and BH_4^- are not likely compatible in the same structure. This is in contrast to a recent computational study that predicted $[\text{NH}_4]^+[\text{BH}_4]^-$ should be an energetically stable Zinc Blende [ZB] structure.¹⁶ However, these conclusions were based on electronic energies only and included neither zero-point vibrational nor thermal corrections. Furthermore, there is no experimental data providing insight into the solid phase structure of $[\text{NH}_4]^+[\text{BH}_4]^-$ or the enthalpy of reaction for hydrogen release that would provide a benchmark for the calculations.

Herein, we report an experimental and computational study to gain insight in to the most stable structure and thermodynamics of dehydrogenation of this H-rich material. In this letter, we show the ammonium borohydride releases > 20 wt % hydrogen in three steps at temperatures < 160 °C and provide evidence that $[\text{NH}_4]^+[\text{BH}_4]^-$ crystallizes at room temperature and standard pressure in a rock salt [RS] structure and not a ZB structure that we previously proposed.¹⁶

Ammonium borohydride was prepared as previously described.¹⁵ The isolated compound does slowly decompose at room temperature but can be stored for longer periods of time in liquid ammonia or at temperatures below –40 °C. Temperature-programmed thermogravimetric analysis (TGA) coupled with differential scanning calorimetry (DSC) and mass analysis (MA) of the volatile products provides insight in to the hydrogen release pathways from ammonium borohydride (Figure 1). The TG/DSC traces reveal three distinct, moderately exothermic, decomposition steps resulting in a mass loss of ca. 21 wt % at temperatures < 160 °C. Mass spectral analysis of the volatile species, under the same reaction conditions (ramped temperature rate of 1 °C/min), shows hydrogen gas being the only major product during the decomposition with only trace amounts of borazine observed during the third dehydrogenation step. Volumetric analysis of the hydrogen released from $[\text{NH}_4]^+[\text{BH}_4]^-$ using a gas buret confirmed the yield of hydrogen, ca. 20 wt %, comparable to the mass loss observed by TGA.

The 6.5% decrease in mass in the first step is consistent with desorption of 1 equiv. of H_2 from $[\text{NH}_4]^+[\text{BH}_4]^-$. It has been reported previously that decomposition of $[\text{NH}_4]^+[\text{BH}_4]^-$ in the solid state yields an amorphous white solid with a composition of $(\text{NBH}_6)_x$ believed to contain structural features comparable to the diammoniate of diborane ($[\text{NH}_3\text{BH}_2\text{NH}_3]^+[\text{BH}_4]^-$ denoted as DADB), whereas decomposition of $[\text{NH}_4]^+[\text{BH}_4]^-$ in the solution phase yields ammonia borane.^{15,17} The differences in reaction channels in the solid and solution phase were not completely understood. To better understand

*Corresponding author.

- (1) Schlapbach, L.; Zuttel, A. *Nature* **2001**, *414*, 353–358.
- (2) Satyapal, S.; Petrovic, J.; Read, C.; Thomas, G.; Ordaz, G. *Catal. Today* **2007**, *120*, 246–256.
- (3) Marder, T. B. *Angew. Chem., Int. Ed.* **2007**, *46*, 8116–8118.
- (4) Chen, P.; Xiong, Z. T.; Luo, J. Z.; Lin, J. Y.; Tan, K. L. *Nature* **2002**, *420*, 302–304.
- (5) Chen, P.; Zhu, M. *Mater. Today* **2008**, *11*, 36–43.
- (6) Grochala, W.; Edwards, P. P. *Chem. Rev.* **2004**, *104*, 1283–1315.
- (7) Custelcean, R.; Jackson, J. E. *Chem. Rev.* **2001**, *101*, 1963–1980.
- (8) He, T.; Xiong, Z. T.; Wu, G. T.; Chu, H. L.; Wu, C. Z.; Zhang, T.; Chen, P. *Chem. Mater.* **2009**, *21*, 2315–2318.
- (9) Heldebrant, D. J.; Karkamkar, A.; Hess, N. J.; Bowden, M.; Rassat, S.; Zheng, F.; Rappe, K.; Autrey, T. *Chem. Mater.* **2008**, *20*, 5332–5336.
- (10) Her, J. H.; Stephens, P. W.; Gao, Y.; Soloveichik, G. L.; Rijssenbeek, J.; Andrus, M.; Zhao, J. C. *Acta Crystallogr., Sect. B* **2007**, *63*, 561–568.
- (11) Hugel, T.; Kuhnelt, M. F.; Lentz, D. *J. Am. Chem. Soc.* **2009**, *131*, 7444–7446.
- (12) Orimo, S. I.; Nakamori, Y.; Eliseo, J. R.; Zuttel, A.; Jensen, C. M. *Chem. Rev.* **2007**, *107*, 4111–4132.
- (13) Ozolins, V.; Majzoub, E. H.; Wolverson, C. *J. Am. Chem. Soc.* **2009**, *131*, 230–237.
- (14) Filinchuk, Y.; Chernyshov, D.; Nevidomskyy, A.; Dmitriev, V. *Angew. Chem., Int. Ed.* **2008**, *47*, 529–532.
- (15) Parry, R. W.; Schultz, D. R.; Girardot, P. R. *J. Am. Chem. Soc.* **1958**, *80*, 1–3.

- (16) Gutowski, M.; Autrey, T. In *Abstracts of Papers of the American Chemical Society*; American Chemical Society: Washington, D.C., 2004; Vol. 227, pp U1088–U1088.
- (17) Parry, R. W.; Shore, S. G. *J. Am. Chem. Soc.* **1958**, *80*, 15–20.

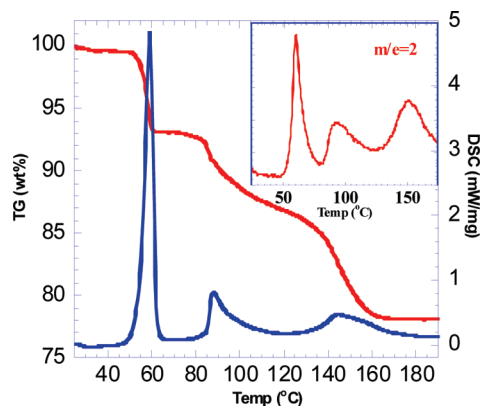


Figure 1. DSC-TGA-MA data for decomposition of ammonium borohydride, $[\text{NH}_4]^+[\text{BH}_4]^-$, heated at $1^\circ\text{C}/\text{min}$, shows three distinct steps for hydrogen release: step 1, $T_d=53^\circ\text{C}$, mass loss 6.5%, ΔH_1 ca. -40 kJ/mol; step 2, $T_d=85^\circ\text{C}$, mass loss 6.0%, ΔH_2 ca. -15 kJ/mol; step 3, $T_d=130^\circ\text{C}$, mass loss 9%, ΔH_3 ca. -13 kJ/mol.

the reaction mechanisms for $[\text{NH}_4]^+[\text{BH}_4]^-$ decomposition we performed a control experiment, where we observed the immediate formation of diammoniate of diborane, DADB, upon mixing NH_3BH_3 with $[\text{NH}_4]^+[\text{BH}_4]^-$ in the solid state at room temperature (see Figure S1 in the Supporting Information). This observation supports the two-step decomposition pathway, where step 1a is the rate limiting reaction between the protonic hydrogens of NH_4^+ with the hydridic hydrogens of BH_4^- to yield NH_3BH_3 (AB) and H_2 , and step 1b, where the nascent AB reacts with $[\text{NH}_4]^+[\text{BH}_4]^-$ to yield DADB and H_2 . As H_2 is the only volatile gas observed in the first decomposition an estimate of the enthalpy of H_2 loss from $[\text{NH}_4]^+[\text{BH}_4]^-$ to form DADB can be inferred, $\Delta H = -40$ kJ/mol as measured from the DSC experiments. The measured enthalpy of hydrogen release is slightly less exothermic than the recently published CCSD(T) calculated enthalpy.^{16,18}

In the subsequent decomposition step beginning at 85°C the DADB, formed from $[\text{NH}_4]^+[\text{BH}_4]^-$ decomposition, releases another equivalent of H_2 with the concomitant formation of polyaminoborane (PAB) at temperatures slightly lower than observed for the decomposition of ammonia borane. In the final step, a third equivalent of H_2 is released from the PAB to yield the polyiminoborane (PIB) at 130°C . A small amount of borazine is observed during this step. The results of the experiments showing the corresponding reaction channel, the decomposition temperature, T_d , and the associated reaction enthalpy for release of hydrogen are summarized in Table 1.¹⁶

Contrary to previous computational studies that suggested a ZB structure for $[\text{NH}_4]^+[\text{BH}_4]^-$ the experimental powder XRD identifies a face centered cubic symmetry (Rock Salt), space group $Fm\bar{3}m(225)$, analogous to the alkali metal borohydrides with comparably sized cations, i.e., K^+ , 137 pm, $a = 6.731$ Å; NH_4^+ , ca. 143 pm, $a = 6.987$ Å; and Rb^+ , 152 pm, $a = 7.029$ Å.¹⁹

Table 1. Corresponding Reaction Channel, Decomposition Temperature, T_d , and Associated Reaction Enthalpy for Release of Hydrogen^a

step	starting material	products	T_d ($^\circ\text{C}$)	ΔH (kJ/mol)
1a	$[\text{NH}_4]^+[\text{BH}_4]^-$	$\text{NH}_3\text{BH}_3 + \text{H}_2$		
1b	$[\text{NH}_4]^+[\text{BH}_4]^- + \text{NH}_3\text{BH}_3$	$[\text{NH}_3\text{BH}_2\text{NH}_3]^+[\text{BH}_4]^- + \text{H}_2$	50	-40
2	$[\text{NH}_3\text{BH}_2\text{NH}_3]^+[\text{BH}_4]^-$	$\text{PAB} + \text{H}_2$	85	-15
3	$\text{PAB} + \text{H}_2$	$\text{PIB} + \text{H}_2$	130	-13

^a Step 3 involves cross-linking, hence the weight loss of $\sim 9\%$.

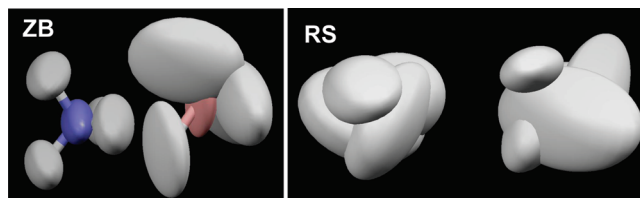


Figure 2. Thermal ellipsoids determined from the ab initio MD trajectory of the zinc blende (ZB, left) and rock salt (RS, right) structures of $[\text{NH}_4]^+[\text{BH}_4]^-$ obtained from a canonical ensemble of configurations at 300 K. The atoms are: N (blue), B (magenta), and H (white). It is seen that the hydrogen atoms are more mobile around both N and B in the rock salt (right) structure compared to those found in ZB (left). Interestingly, the hydrogens around the B atoms are more mobile than those around the N atoms in ZB (left) (see Figure S2 in the Supporting Information for a more quantitative comparison).

XRD profile are calculated based on the 220 reflections and indicate $a = 6.978$ Å with a unit cell volume of 339.776 Å³ ($Z = 4$) and the calculated density of 0.642 g/cm³. Additionally, the Raman spectrum of the freshly prepared sample shows two intense modes corresponding to the N–H symmetric stretch at 3118 cm⁻¹ and the B–H symmetric stretch at 2295 cm⁻¹, as shown Figure S3 of the Supporting Information.^{20,21} The solid state MAS ¹¹B NMR spectrum shows only a single sharp resonance at -35 ppm as in Figure S4 of the Supporting Information.

As indicated previously, exploring the stability of the structure of $[\text{NH}_4]^+[\text{BH}_4]^-$ is complicated by the fact that the RS structure is very close in energy to the ZB structure. Previous computational results found the ZB structure to be the more energetically favorable compared to the RS;¹⁶ however, experimentally, only the RS structure is found. Thus, we consider only the RS and ZB structures. Figure 2 shows the calculated thermal ellipsoids for the ZB and RS structures determined from our ab initio MD (AIMD) simulations using a super cell containing 32 $[\text{NH}_4]^+[\text{BH}_4]^-$ molecular ion pairs averaged over 6 ps (post-equilibration) with a 0.5 fs time step. The thermal ellipsoids represent correlations in the fluctuations in the atomic coordinates about minima on the potential energy surface. This analysis is justified as long as the atomic motions are local and no jumps (or rotations) are sampled. Our simulations are long enough to sample the large atomic fluctuations, but short enough that we do not see jumps or rotations. The

(18) Dixon, D. A.; Gutowski, M. *J. Phys. Chem. A* **2005**, *109*, 5129–5135.

(19) Renaudin, G.; Gomes, S.; Hagemann, H.; Keller, L.; Yvon, K. *J. Alloys Compd.* **2004**, *375*, 98–106.

(20) Hagemann, H.; Gomes, S.; Renaudin, G.; Yvon, K. *J. Alloys Compd.* **2004**, *363*, 126–129.

(21) Taylor, R. C.; Schultz, D. R.; Emery, A. R. *J. Am. Chem. Soc.* **1958**, *80*, 27–30.

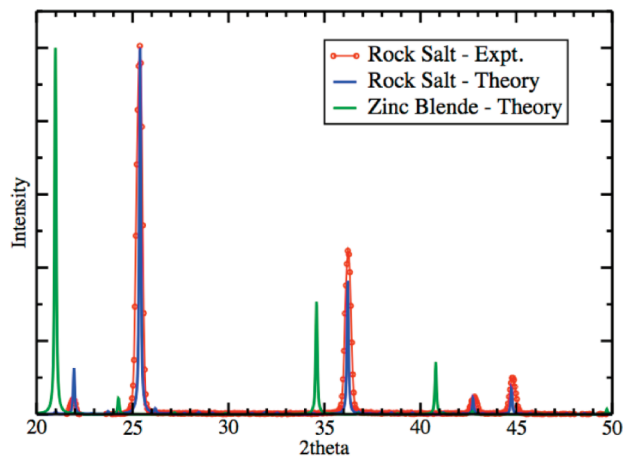


Figure 3. Comparison of the experimental (rock salt) and theoretical (RS and ZB) XRD patterns for $[\text{NH}_4]^+[\text{BH}_4]^-$ at 300 K. There is excellent agreement between experiment and theory for the RS pattern. The ZB XRD is shown as a prediction and for comparison.

quantification of the thermal ellipsoids is standard and follows the conventions equivalent to the B-matrix formalism used in crystallography. It is seen in Figure 3 that the hydrogen atoms are more mobile around both N and B in the RS (right) structure compared to those found in ZB (left). Interestingly, the hydrogens around the B atoms are more mobile than those around the N atoms in ZB (left). In Figure S2 in the Supporting Information, we show the distribution of the largest principal moment $U^{1/2}$ of the thermal ellipsoids (in Angstroms) determined from the dynamics trajectory. Here the covariance matrix \mathbf{U} was constructed from the coordinates for each atom over the total length of the trajectory. It is clear that, on average, the RS (right) principal moments of the thermal ellipsoids are larger than those found in the ZB (left) structure. But, they do overlap significantly. In Figure S5 of the Supporting Information, we show the potential energy distribution for both RS and ZB structures. The potential energy difference between RS and ZB is $\Delta E = 128.9$ kJ/mol, favoring the ZB structure. However, the potential energy difference alone does not determine the most stable phase; the most stable phase is determined from the phase having the lowest free energy.

Direct calculation of the anharmonic Helmholtz free energy is quite challenging and remains a subject of future work in the statistical mechanics of solids. Here, we simply make the quasiharmonic approximation²² where the essential vibrational modes are determined from the covariance matrix, which is equivalent to the second moment matrix constructed from the fluctuations of the atomic positions about their average position as determined from the AIMD trajectory. The effective force constant matrix (\mathbf{K}) is related to the covariance matrix (\mathbf{U}) by $\mathbf{K} = k_B T \mathbf{U}^{-1}$. Because the effective force constant matrix and the covariance matrix share common eigenvectors (\mathbf{L}), the effective eigenfrequencies (ω_{eff}) are determined from the mass-weighted

inverse of the covariance matrix using the equation $m^{-1/2} k_B T \mathbf{U}^{-1} m^{-1/2} \mathbf{L} = \omega_{\text{eff}}^2 \mathbf{L}$. Using these frequencies, we can estimate their contribution to the entropy and hence the Helmholtz free energy of the RS versus ZB structures. The vibrational contribution to the Helmholtz free energy for a particular mode is given by $A = k_B T \sum_{\text{modes}} \ln[2 \sinh(\hbar \omega_{\text{eff}} / 2 k_B T)]$. Summing over all modes yields an estimated Helmholtz free energy for the RS and ZB structures. Notably, the larger entropy contribution in the RS structure changes the relative stability of the two structures, predicting the free energy of the RS structure to be lower than that of the ZB structure by ca. 18.4 kJ/mol.²³ These results are consistent with preliminary quasi-harmonic thermodynamic analysis derived from dynamical correlation functions. An analysis of this approach, its convergence, and general approaches to calculate solid-state free energies will be the subject of future investigations.

A comparison of the experimental and theoretical X-ray powder diffraction (XRD) pattern of the RS structure of $[\text{NH}_4]^+[\text{BH}_4]^-$ is shown in Figure 3. There is excellent agreement between experiment and theory for the RS pattern. The ZB XRD is shown as a prediction and for comparison. The simulated diffraction pattern was obtained using the average positions and thermal ellipsoids representing the motion of the ions at 300 K.

In summary we demonstrated that ammonium borohydride, a unique compound that provides storage of hydrogen on both the cation NH_4^+ and the anion BH_4^- , releases 20 wt % of hydrogen at temperatures lower than 160 °C. Mechanistically, hydrogen release is shown to proceed through a multi-step pathway leading to the formation of AB, DADB, PAB, and PIB consecutively. The most stable phase at room temperature determined by powder XRD is shown to be a FCC framework with rock-salt type structure. AIMD theory shows that the RS and ZB structures are very close in energy, however, the greater disorder of hydrogen leads to a lower free energy in the RS structure. Predicting temperature-dependent thermodynamic stabilities from simulations remains a challenge. More effort is required to better understand the accuracy and limitations of various methods used to obtain free energies such as: the AIMD functional employed, anharmonic/temperature effects, phonon dispersion, polymorphs, and the multiple minima problem. Future work will focus on approaches to stabilize ammonium borohydride, the compound with the large hydrogen storage density (ca. 244 g H_2 /kg and 154 g H_2 /L), at ambient temperatures.

Acknowledgment. This work was supported support from the U.S. Department of Energy, Office of Basic Energy, Division of Chemical Sciences, Biosciences and Geosciences. PNNL is operated for the DOE by Battelle.

Supporting Information Available: Experimental section and additional figures (PDF). This material is available free of charge via the Internet at <http://pubs.acs.org>.

(22) Madsen, A. O.; Larsen, S. *Angew. Chem., Int. Ed* **2007**, *46*, 8609–8613.

(23) $\Delta A = A(\text{RS}) - A(\text{ZB}) = \Delta E - T\Delta S = 30.8 - 172.1 = -141.3$ kcal for 32 pair cell.